Arm-Free Paraplegic Standing—Part I: Control Model Synthesis and Simulation

Zlatko Matjačić and Tadej Bajd, *Senior Member, IEEE*

***Abstract*— The following paper is the first part of our investigation into the feasibility of arm-free paraplegic standing. A novel control strategy for unsupported paraplegic standing which utilizes the residual sensory and motor abilities of the thoracic spinal cord injured subjects is proposed. The strategy is based on voluntary and reflex activity of the paraplegic person's upper body and artificially controlled stiffness in the ankles. The knees and hips are maintained in an extended position by functional electrical stimulation (FES). The analysis of a linearized double inverted pendulum model revealed that with properly selected ankle stiffness the system can be easily stabilized. We developed a closed-loop double inverted pendulum model including a neural system delay, trunk muscles dynamics, body segmental dynamics and linear quadratic regulator (LQR) optimal controller. Through simulations of the closed-loop model two different strategies for disturbance rejection were explained. We investigated the capability of the closed-loop model to reject disturbances, imposed at the ankle joint (in anterior and posterior directions) for various stiffness levels and neural system delays in the presence of biomechanical constraints. By limiting permissible excursions of the center of pressure, we found out that the length of the foot is the most important constraint, while the strength of the trunk muscles is not of major importance for successful balancing. An ankle stiffness of approximately 10 Nm/$^{\circ}$ suffices for arm-free standing of paraplegic subjects.**

***Index Terms*—Optimal control, postural strategies, underactuated biomechanical systems, unsupported paraplegic.**

I. Introduction

A. Problem Statement

ARM-SUPPORTED standing and limited crutch or walker assisted walking can be restored in spinal cord injured (SCI) persons by means of functional electrical stimulation (FES) [1]. The ability to stand is of great importance for SCI subjects because it enables them to perform many daily activities and, more importantly, it is a prerequisite for walking. Standing of SCI persons is additionally beneficial because it has many therapeutic and psychological effects [1], [2]. It prevents joint contractures, improves the cardiovascular response, reduces the incidence of developing pressure sores, reduces the incidence of bladder infections, decreases the level of spasticity, decreases bone loss as well as improves the self-image of a subject.

Manuscript received September 16, 1997; revised January 15, 1998 and March 9, 1998. This work was supported by the Republic of Slovenia Ministry of Science and Technology and European Commission (BIOMED 2, SENSATIONS-PL 950897).

The authors are with the Faculty of Electrical Engineering, University of Ljubljana, 1000 Ljubljana, Slovenia.

Publisher Item Identifier S 1063-6528(98)03846-4.

Paraplegia may result in a complete loss of the somatosensory and motor functions of the lower extremities, but also lead in exaggerated reflex activity and joint contractures. Trying to restore the lost locomotion functions after SCI is, therefore, a challenging task [3]. Accurate models and model parameters may be needed in order to achieve adequate performance of rehabilitative devices or methods. Furthermore, feedback control usually requires accurate, reliable and calibrated sensors. When coping with such a delicate task as unsupported standing of a paraplegic person, where the body is inherently unstable, system parameters are changing (primarily due to muscle fatigue) and the achievable stability margins of the closed-loop system are very narrow, we would like to use adaptive control and on-line identification of the changing parameters of the system, in order to achieve robust stability.

As a consequence in present FES aided standing, paraplegics maintain an upright posture by means of usually substantial arm support, thus acting as an adaptive controller themselves. In the most usual FES-assisted posture, the knee joints are locked by the open-loop FES of knee extensor muscles, the hips are hyperextended (C posture) while the ankles are free to move. Improved standing balance can be achieved by adding the stimulation of hip extensors and abductors [1]. Due to fatigue of electrically activated knee extensors, a paraplegic can usually only stand in the manner for a few minutes.

In order to prolong FES assisted standing of paraplegic subjects, Kralj *et al.* [4] introduced the concept of *posture switching* in which several different postures are adopted cyclically. Each posture requires FES of different leg muscles, thus reducing the average muscle fatigue considerably. The investigations on closed-loop [5] and "finite-state artificial control" [6] stabilization of knee joints were also undertaken in order to overcome the fatigue of the electrically stimulated muscle.

Efforts to analyze the possibilities of achieving arm-free paraplegic standing have been undertaken. Jaeger [7] has developed an inverted pendulum model of unsupported standing. He has shown that the pendulum can be asymptotically stabilized by a proportional-derivative (PD) controller, at least for nominal plant parameters. Donaldson [8] has also studied the behavior of a single link model controlled by an ankle controller. He proposed a cascade controller where the outer loop stabilizes the inverted pendulum while the inner loop enhances the ankle torque tracking. Munih *et al.* [9], [10] have shown in controlled laboratory conditions that the latter approach can be accomplished with a paraplegic subject. In all four papers, the authors assumed inactivity of the upper body

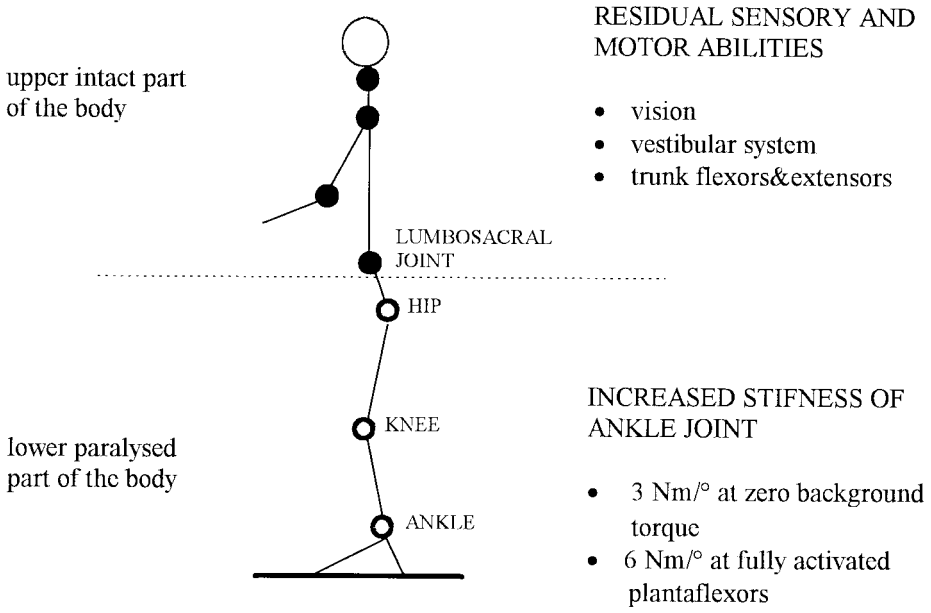

Fig. 1. Paraplegic subject after thoracic SCI. The upper part of figure shows residual sensory and motor abilities, while lower part displays properties of paralyzed ankle joints.

although, usually this is largely under the voluntary control of the standing subject.

However, there is little benefit for the paraplegic subject's functionality if his upper body has to remain still in order to allow the artificial controller of lower limbs to maintain a standing posture. Clearly, the main control problem, in unsupported paraplegic standing, is how to integrate the upper body voluntary activity with the artificially controlled paralyzed lower extremities, in a manner that provides an adaptive and robust global control system.

B. Proposed Control Scheme

Paraplegic subjects, suffering from complete thoracic spinal cord lesions (T4–T12), have preserved visual and vestibular sensory systems and motor abilities of arms and neck (Fig. 1). Voluntary control of trunk muscles is only partially preserved and depends on the level of lesion. Matjačić *et al.* [11] have shown that the trunk flexor and extensor muscle groups in some paraplegic subjects are capable of generating isometric and isokinetic torques around the lumbosacral joint (L5–S1, [12]) that are comparable to the abilities of normal subjects. The studies of Munih *et al.* have shown increased stiffness (passive and intrinsic) in a paraplegic ankle joint [9], compared to the stiffness of the ankle joint in an intact subject [10], both measured under the conditions of electrically activated plantarflexor muscle group. Without activation, the stiffness in the intact subject was 1 Nm/°, and in the paraplegic subject 3 Nm/°. At full activation of the plantarflexor muscle group, the stiffness values were 4 and 6 Nm/°, respectively (Fig. 1).

It has been shown that a normal person, who is exposed to a sudden perturbation in the posterio-anterior direction, typically responds by deploying either an ankle- or hip-balancing strategy, or a combination of both [13]. Considering the residual sensory and motor abilities of a thoracic paraplegic, we can observe some similarities to motor resources used by an intact subject in the hip-balancing strategy. A normal subject, while standing, predominantly responds to larger unexpected disturbances through hip and trunk movements in a feedback manner, while keeping his knee joints in an extended position. Ankle agonists and antagonists show increased activity, resulting in increased stiffness of the joint [14]. Anyone using hip-balancing strategy behaves like a double inverted pendulum.

Similar balancing activity might also be obtained in a paraplegic subject. If the knees and hips of a paraplegic subject are locked in extended positions, either by open- or closed-loop stimulation of the knee and hip extensors, while simultaneously the paralyzed ankles exhibit an adequate stiffness, then it might be possible for a paraplegic to successfully balance his body by the voluntary and reflex activity of his preserved trunk flexor and extensor muscles. The question addressed in this paper is what value of ankle stiffness is desired?

In Fig. 2, the proposed control scheme for arm-free paraplegic standing is displayed. The artificial controllers are simple SISO (single input, single output) controllers and we assume that the central nervous system (CNS) integrates the behavior of the entire system and adapts to changes in the system parameters (movement of arms and head, neurophysiological delays) as well as the degradation of the performance of the artificial controllers, due to the fatigue of the stimulated muscles. Apart from visual and vestibular sensors, we may also use artificial sensory cognitive feedback to indicate the status of the paralyzed lower part of the body.

In this approach, the residual upper body sensory and motor abilities as well as the brain, are included in a postural loop. This makes standing control intelligent by including the adaptive and learning capabilities of CNS. It is, therefore, sensible to include such an excellent controller in a global control scheme while trying to restore paraplegic arm-free standing. This control scheme is additionally attractive because

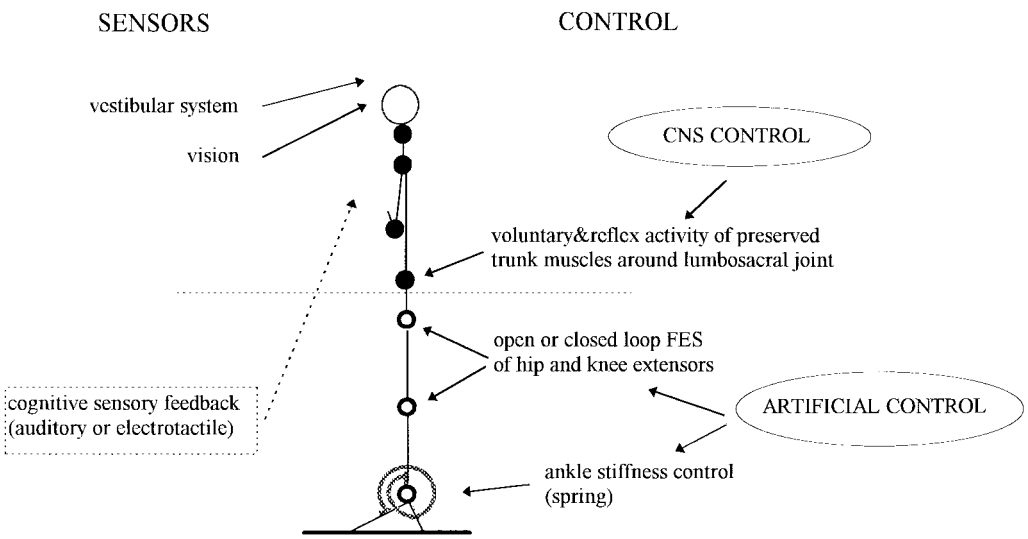

Fig. 2. The proposed control scheme for unsupported paraplegic standing. The knees and hips are assumed to be locked by FES. Stiffness in the ankle joints is composed from passive, intrinsic, reflex and artificially produced stiffness (by FES or springs). The paraplegic subject receives sensory information from vestibular and visual systems and maintains standing by voluntary and reflex activity of preserved trunk muscles. Cognitive sensory feedback may also be utilized. The CNS integrates the control of the upper, nonparalyzed part of the body with, artificially controlled lower extremities.

the desired ankle stiffness can easily be obtained by means of springs, mounted in the shoes.

C. Objectives

This pair of papers describe a theoretical and experimental investigation of the proposed scheme of arm-free paraplegic standing in complete SCI subjects. The objective of Part I is to derive a simplified closed-loop model which accounts for all the important properties and constraints. Through analysis of the open-loop model properties, and computer simulations of the closed-loop model, we obtained an insight into the feasibility and limitations of the concept which were indispensable in the design of the experimental investigation, described in Part II.

II. Mathematical Model

There are numerous questions about the proposal that need to be answered before attempting to implement such standing. We need to know which value of ankle stiffness is the most appropriate; what are the magnitudes of lumbosacral torque needed for maintaining standing and rejecting disturbances; which biomechanical constraints limit the postural activity of a standing person; and what is the influence of inevitable neural delay, which is the time taken for sensing and processing in the brain and the issuing of control signals to trunk muscles.

In the following section we describe a linear dynamic model. Several authors [15]–[21] have modeled the complex voluntary and reflex postural activity of a standing man by a linear plant and linear feedback controllers. Experiments have shown a considerable agreement with the trajectories predicted by these linear models.

Our linear model is composed of four components: the body segmental dynamics, the CNS delay, the trunk muscle activation properties, and the linear controller dynamics. Here, controller dynamics refer to a natural CNS controller (Fig. 2).

A. Body Segmental Dynamics

The body segmental model is planar and describes movements of the mechanical structure in the sagittal plane. It consists of two links and two frictionless hinge joints, each having one degree of freedom (Fig. 3). The lower paralyzed link represents the shanks, thighs and pelvis. The extended positions of the knee and hip joints are assumed to be maintained by stimulation of the knee- and hip-extensor muscles. The stiffness in both ankles is assumed to be controlled via the closed-loop FES of ankle dorsal and plantar-flexors or by a mechanical spring. It is also assumed that the conditions in both lower extremities are identical, therefore, both legs and the pelvis are lumped in a single lower link. The upper link represents the head, arms, and trunk (HAT). Finally, the arms of the standing subject are folded at the chest.

It is further assumed that the center of masses of each segment lies on the line connecting two adjacent joints and that the position of the center of rotation in the lumbosacral joint does not change. The nonlinear equations of motion were derived by the Newton–Euler method

$$\begin{aligned}\tau_1 = &-m_2 g l_{c2} \sin\psi - (m_1 g l_{c1} + m_2 g l_1)\sin\theta \\ &- m_2 l_1 l_{c2} \sin(\psi-\theta)(\dot{\psi}^2 - \dot{\theta}^2) \\ &+ [J_2 + m_2 l_{c2}^2 + m_2 l_1 l_{c2}\cos(\psi-\theta)]\ddot{\psi} \\ &+ [J_1 + m_1 l_{c1}^2 + m_2 l_1^2 + m_2 l_1 l_{c2}\cos(\psi-\theta)]\ddot{\theta}. \quad (1)\\ \tau_2 = &-m_2 g l_{c2}\sin\psi + m_2 l_1 l_{c2}\sin(\psi-\theta)\dot{\theta}^2 \\ &+ [J_2 + m_2 l_{c2}^2]\ddot{\psi} + m_2 l_1 l_{c2}\cos(\psi-\theta)\ddot{\theta}. \quad (2)\end{aligned}$$

All symbols used in (1) and (2) are defined and explained in Fig. 3. These equations are subject to biomechanical constraints. The length of the foot places biomechanical constraints on the torque, that can act around the ankle joint, without lifting the heels or toes.

Fig. 4 shows the torque and forces acting on the foot and the resulting center of pressure (COP) as shown

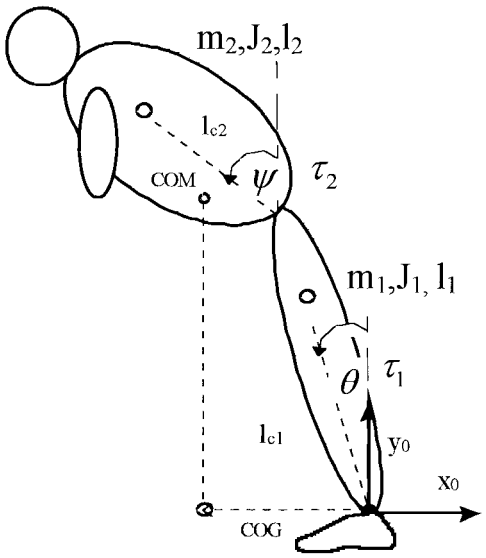

Fig. 3. Double link inverted pendulum model of the paraplegic standing. Centers of masses of both links and center of mass (COM) of the entire body and its vertical projection COG together with the distances from joints to centers of masses (l_{c1}, l_{c2}) and lengths of upper and lower links (l_1, l_2) are shown. The angles (θ—ankle joint, ψ—lumbosacral joint) are measured with respect to the vertical line. τ_1, τ_2 are the net torques produced by FES of muscles or mechanical spring in the ankle joint and by voluntary activation in the lumbosacral joint. m_1, m_2 are the masses of both links and J_1, J_2 are the moments of inertia around the mass centers of each link.

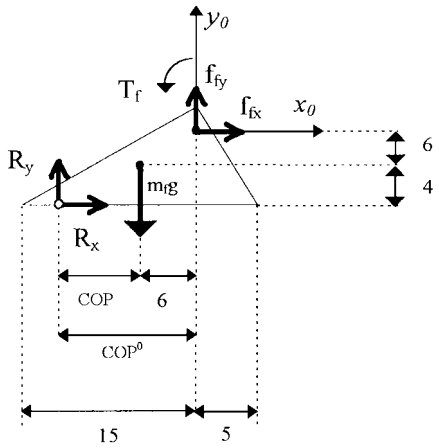

Fig. 4. Center of pressure COP^0, resulting from the torque and forces acting on the foot is expressed in the base coordinate system (x_0, y_0). Force $\vec{f}_f$ and torque T_f are exerted on the foot by a lower link. R_x and R_y are components of the ground reaction force. The dimensions of the foot are given in [cm].

in (2a) at the bottom of the page where COP, as defined in Fig. 4, is determined by the equality:

$$\text{COP} = \frac{T_f + 0.06 \cdot f_{fy} + 0.04 \cdot R_x - 0.06 \cdot f_{fx}}{R_y}.$$

The center of pressure (COP^0), expressed in the base coordinate frame (x_0, y_0) is

$$\text{COP}^0 = -0.06 - \text{COP}. \tag{3}$$

The following inequality, which poses the first constraint on the dynamics of the mechanical model, must be satisfied:

$$-0.15 < \text{COP}^0 < 0.05. \tag{C1}$$

The dimensions of the foot were adapted from [22]. The excursions of the center of gravity (COG) of the standing person are also limited to the same area under the foot. Once the COG extends beyond the foot, the body cannot exert the appropriate torques to counteract gravity, and cannot remain stable without either receiving an external stabilizing force or taking a step [23]

$$-0.15 < \text{COG} < 0.05. \tag{C2}$$

The third constraint results from the strength of the trunk muscles which determine the maximal torque produced in the lumbosacral joint. In our previous work [11] we examined the strength of the trunk muscles in a normal and three paraplegic subjects under isometric and isokinetic (velocity 30°/s) conditions. The maximal torque produced by trunk flexors and trunk extensors in the normal subject was 120 and 130 Nm, respectively. The trunk strength of paraplegic subjects was within 20–80% of these values. In this paper we examined the closed-loop performance of the model at three different values for the lumbosacral torque constraint (C3), namely 100, 50, and 20% of the normal subject's torque.

The subject's total mass, and the frictional properties of the contact with the floor, determine the upper bound on the magnitude of the shear force at the ground, which in turn determines the upper bound on the torque produced at the lumbosacral joint (C4). We will assume that the constraint (C4) is met at all times.

B. Dynamical Coupling Index and Equilibrium States of the Model

The ankle joint exhibits passive mechanical impedance behavior. The torque acting around the ankle joint consists of the elasticity and viscous damping

$$\tau_1 = -K \cdot \theta - B_G \dot{\theta}. \tag{4}$$

The stiffness K is a variable which may be varied in order to achieve optimal performance. K is composed from passive, intrinsic and reflex joint stiffness [24] as well as artificially produced stiffness which can be obtained either by FES of

$$\vec{f}_f = \begin{pmatrix} f_{fx} \\ f_{fy} \\ f_{fz} \end{pmatrix} = \begin{pmatrix} -(m_1 l_{c1} + m_2 l_1)\sin\theta \cdot \dot{\theta}^2 - m_2 l_{c2} \sin\psi \cdot \dot{\psi}^2 + m_2 l_{c2} \cos(\psi - \theta)\ddot{\psi} + (m_1 l_{c1} + m_2 l_1)\cos\theta \cdot \ddot{\theta} \\ -m_1 g - m_2 g + m_2 l_{c2} \cos\psi \cdot \dot{\psi}^2 \\ +m_2 l_{c2} \sin\psi \cdot \ddot{\psi} + (m_1 l_{c1} + m_2 l_1)\cos\theta \cdot \dot{\theta}^2 + (m_1 l_{c1} + m_2 l_1)\sin\theta \cdot \ddot{\theta} \\ 0 \end{pmatrix}$$

$$T_f = -\tau_1,\ R_x = -f_{fx},\ R_y = -f_{fy} - m_f g. \tag{2a}$$

ankle joint agonists and antagonists or by a mechanical spring. The viscous damping coefficient B_G represents the passive velocity-dependent properties of the joint. The numerical value of B_G in a spastic paraplegic joint in isotonic conditions was found to be 1 Nms/rad [25]. In the following simulations we used the value of 2 Nms/rad, each leg contributing one half of the viscous damping. By substituting τ_1 from (4) in the double inverted pendulum equation (1), it can be observed that the only input of the model is lumbosacral torque τ_2, which is under the control of CNS.

Our model has only one actuator and two joints what makes it an underactuated system. Extensive studies were undertaken in the field of robotics to develop theoretical tools allowing controllability analysis of the underactuated systems [26], [27]. Dynamic equations (1), (2), (4) can be written in the following compact form:

$$\underline{\underline{M}}(\underline{q})\ddot{\underline{q}} + \underline{C}(\underline{q}, \dot{\underline{q}}) = \underline{\tau} \tag{5}$$

where $\underline{\underline{M}}(\underline{q})$ is the inertia matrix, $\underline{C}(\underline{q}, \dot{\underline{q}})$ is a vector of velocity and gravity terms while the state vector and input vector are defined as follows:

$$\underline{q} = \begin{bmatrix} \theta \\ \psi - \theta \end{bmatrix} \text{ and } \underline{\tau} = \begin{bmatrix} 0 \\ \tau_2 \end{bmatrix}.$$

Equation (5) can be written in a form that separates the passive and active terms of the double inverted pendulum model where $q_p = \theta$ and $q_a = \psi - \theta$, $M_{pp} = M_{11}$, $M_{pa} = M_{12}$, $M_{ap} = M_{21}$, $M_{aa} = M_{22}$, $C_p = C_1$, $C_a = C_2$

$$\begin{bmatrix} M_{pp} & M_{pa} \\ M_{ap} & M_{aa} \end{bmatrix} \begin{bmatrix} \ddot{q}_p \\ \ddot{q}_a \end{bmatrix} + \begin{bmatrix} C_p \\ C_a \end{bmatrix} = \begin{bmatrix} 0 \\ \tau_2 \end{bmatrix}. \tag{6}$$

A dynamic coupling index ρ_c [26] is defined as

$$\ddot{q}_p = \rho_c \ddot{q}_a \tag{7}$$

where

$$\rho_c = -M_{pp}^{-1} M_{pa}$$
$$M_{pp} = J_1 + J_2 + m_1 l_{c1}^2 + m_2 l_1^2 + m_2 l_{c2}^2 + 2 m_2 l_1 l_{c2} \cos(q_2)$$
$$M_{pa} = J_2 + m_2 l_{c2}^2 + m_2 l_1 l_{c2} \cos(q_2).$$

The dynamic coupling relates the acceleration in the unactuated ankle to the acceleration in the active lumbosacral joint. The dynamic coupling indexes for four different sets of model parameters are given in Table I.

In the first set, both links have the same parameters; in the second set, the first link's mass and moment of inertia are larger than the second link; in the third set, the values of masses and moments of inertia are the opposite of the second set; while the fourth set is identical to the first one with the exception of the first link length, which is shorter for 0.2 m. It can be seen that the distribution of masses and moments of inertia among the two links has a small influence on the dynamic coupling index, while the length of the first link has a considerable influence. From an objective biomechanical viewpoint, this result suggests that two subjects of the same height and different body weights will find balancing equally difficult, while smaller subjects will find it easier. The negative sign of the dynamic coupling indexes in Table I means that the acceleration in the lumbosacral joint generates acceleration in the opposite direction at the ankle.

TABLE I
DYNAMIC COUPLING INDEXES FOR FOUR DIFFERENT SETS OF MODEL PARAMETERS

Set	Double inverted pendulum parameters	Dynamic coupling index
1	$m_1 = m_2 = 40kg, l_1 = l_2 = 0.9m, l_{c1} = l_{c2} = 0.45m, J_1 = J_2 = 3kgm^2$	-0.31
2	$m_1 = 50kg, m_2 = 30kg l_1 = l_2 = 0.9m, l_{c1} = l_{c2} = 0.45m,$ $J_1 = 3.5kgm^2, J_2 = 2.5kgm^2$	-0.29
3	$m_1 = 30kg, m_2 = 50kg l_1 = l_2 = 0.9m, l_{c1} = l_{c2} = 0.45m,$ $J_1 = 2.5kgm^2, J_2 = 3.5kgm^2$	-0.33
4	$m_1 = m_2 = 40kg, l_1 = 0.7m, l_2 = 0.9m, l_{c1} = l_{c2} = 0.45m, J_1 = J_2 = 3kgm^2$	-0.37

Underactuated systems cannot assume arbitrary states. Of special interest are the equilibrium states of the double inverted pendulum model. Equilibrium is defined as a system configuration where $\ddot{\theta} = \ddot{\psi} = \dot{\theta} = \dot{\psi} = 0$ and from (2) and (4) it follows:

$$\psi_0 = \arcsin\left[-\frac{(m_1 g l_{c1} + m_2 g l_1)\sin(\theta_0) - K\theta_0}{m_2 g l_{c2}}\right] \tag{8}$$

and from (6)

$$\tau_{20} = -m_2 g l_{c2} \cdot \sin(\psi_0). \tag{9}$$

Given a particular ankle angle θ_0 and ankle stiffness K, the corresponding equilibrium lumbosacral angle ψ_0 can be determined from (8). This equation gives a family of equilibrium points around which the double inverted pendulum structure can be controlled [Fig. 5(a)]. From (9), we can calculate the equilibrium torque that needs to be generated by the trunk muscles.

The following numerical values of a standing subject's parameters, adapted from [22], were used in the calculation of equilibrium states and will be used in further analysis:

$$m_1 = 37.12 \text{ kg}, m_2 = 42.88 \text{ kg}, l_1 = 0.95 \text{ m}, l_{c1} = 0.7 \text{ m},$$
$$l_{c2} = 0.42 \text{ m}, J_1 = 3.5 \text{ kgm}^2, J_2 = 2.5 \text{ kgm}^2.$$

Equilibrium states of the mechanical model can be divided into three groups of postures as follows:

1) forward posture [$\theta_0 > 0$, Fig. 5(b)];
2) upright posture [$\theta_0 = 0$, Fig. 5(c)];
3) backward posture [$\theta_0 < 0$, Fig. 5(d)].

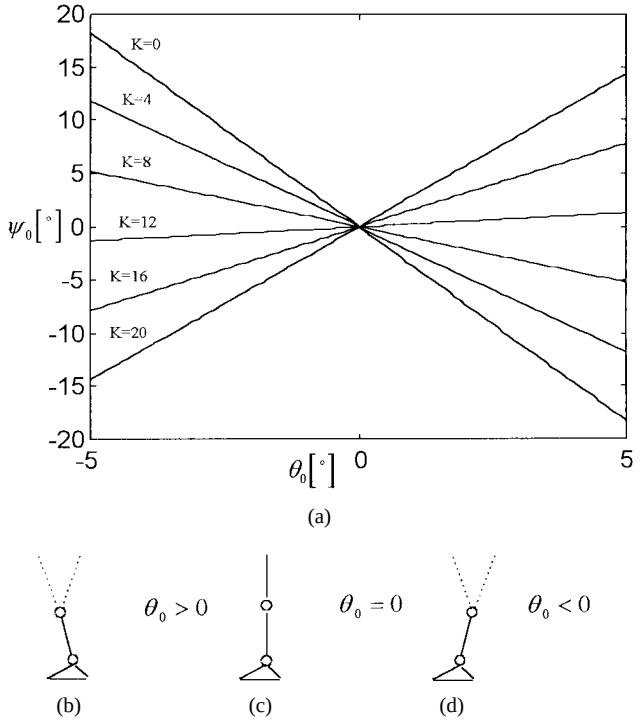

Fig. 5. (a) Family of equilibrium curves depending on ankle stiffness K which is given in [Nm/°]. All feasible postures can be divided into three groups: (b) forward posture, (c) upright posture, and (d) backward posture.

Values of the equilibrium lumbosacral angle ψ_0 in the forward and backward postures depend on the value of ankle stiffness K. From (8) and Fig. 5 it can be redrawn that such a value of stiffness K exists, where the equilibrium lumbosacral angle is approximately zero ($\psi_0 = 0$) regardless of the ankle angle values θ_0. In our case this is true for the approximate stiffness value $K_v = 11.2$ Nm/° where subscript v denotes the vertical.

C. Analysis of the Linearized Model

As the body dynamics during standing have been demonstrated to be fairly linear [21] and since the objective of the paraplegic subject's standing is to maintain a selected posture, we can linearize the double inverted pendulum model. Linearizing (5) around a selected posture (θ_0, ψ_0, τ_{20}) and assuming a quasistatic motion where $\dot{\theta}^2 = 0$, $\dot{\psi}^2 = 0$, $\sin(\alpha) = \alpha$ and $\cos(\alpha) = 1$, the following state space linearized notation can be written:

$$\begin{aligned} \dot{\underline{x}} &= \underline{\underline{A}}\underline{x} + \underline{B}u \\ y &= \underline{\underline{C}}\underline{x} + \underline{D}u \end{aligned} \tag{10}$$

where

$$\underline{\underline{A}} = \begin{bmatrix} 0 & 1 & 0 & 0 \\ \frac{c\cdot f}{\Delta} & -\frac{B_G\cdot f}{\Delta} & \frac{d\cdot f - b\cdot d}{\Delta} & 0 \\ 0 & 0 & 0 & 1 \\ -\frac{c\cdot e}{\Delta} & \frac{B_G\cdot e}{\Delta} & \frac{d\cdot a - e\cdot d}{\Delta} & 0 \end{bmatrix},$$

$$\underline{B} = \begin{bmatrix} 0 \\ -\frac{b}{\Delta} \\ 0 \\ \frac{a}{\Delta} \end{bmatrix}, \quad \underline{\underline{C}} = \begin{bmatrix} 1 & 0 & 0 & 0 \\ 0 & 1 & 0 & 0 \\ 0 & 0 & 1 & 0 \\ 0 & 0 & 0 & 1 \end{bmatrix},$$

$$\underline{D} = \begin{bmatrix} 0 \\ 0 \\ 0 \\ 0 \end{bmatrix}, \quad \Delta = a\cdot f - b\cdot e$$

$$\begin{aligned} a &= J_1 + m_1 l_{c1}^2 + m_2 l_1^2 + m_2 l_1 l_{c2} \\ b &= J_2 + m_2 l_{c2}^2 + m_2 l_1 l_{c2} \\ c &= m_1 g l_{c1} + m_2 g l_1 - K \\ d &= m_2 g l_{c2} \\ e &= m_2 l_1 l_{c2} \\ f &= J_2 + m_2 l_{c2}^2 \end{aligned}$$

$$\underline{x} = \begin{bmatrix} \theta - \theta_0 \\ \dot{\theta} \\ \psi - \psi_0 \\ \dot{\psi} \end{bmatrix}, u = T_2 + T_{20}.$$

The system described by (10) is controllable and observable. It can be further described by the following two transfer functions that are more appropriate for the study of the properties of the open-loop model seen in (11) shown at the bottom of the page.

Both transfer functions have two zeros and four poles. The stiffness of the ankle joint determines the location of zeros and poles in the complex plane. From both transfer functions it can be seen that the body segmental dynamics consists of two coupled univariable subsystems. By dividing one transfer function with the other, the relation between the ankle and lumbosacral angle can be obtained

$$G_{\theta\psi}(s) = \frac{\Theta(s)}{\Psi(s)} = \frac{d - bs^2}{as^2 + B_G s - c}. \tag{12}$$

Fig. 6 shows the location of two zeros and four poles for the three different values of ankle stiffness. With no ankle stiffness at all, both transfer functions $G_\theta(s)$ and $G_\psi(s)$ have two poles in the right-half plane (RHP) and two stable poles. One zero is in the left-half plane (LHP) while the other is in the RHP. The resulting system is unstable and has nonminimum-phase. Furthermore, in both transfer functions the RHP zero lies

$$\begin{aligned} G_\theta(s) &= \frac{\Theta(s)}{U(s)} = \frac{d - bs^2}{\Delta s^4 + f\cdot B_G s^3 + (e\cdot d - a\cdot d - c\cdot f)s^2 - d\cdot B_G s + c\cdot d} \\ G_\psi(s) &= \frac{\Psi(s)}{U(s)} = \frac{as^2 + B_G s - c}{\Delta s^4 + f\cdot B_G s^3 + (e\cdot d - a\cdot d - c\cdot f)s^2 - d\cdot B_G s + c\cdot d} \end{aligned} \tag{11}$$

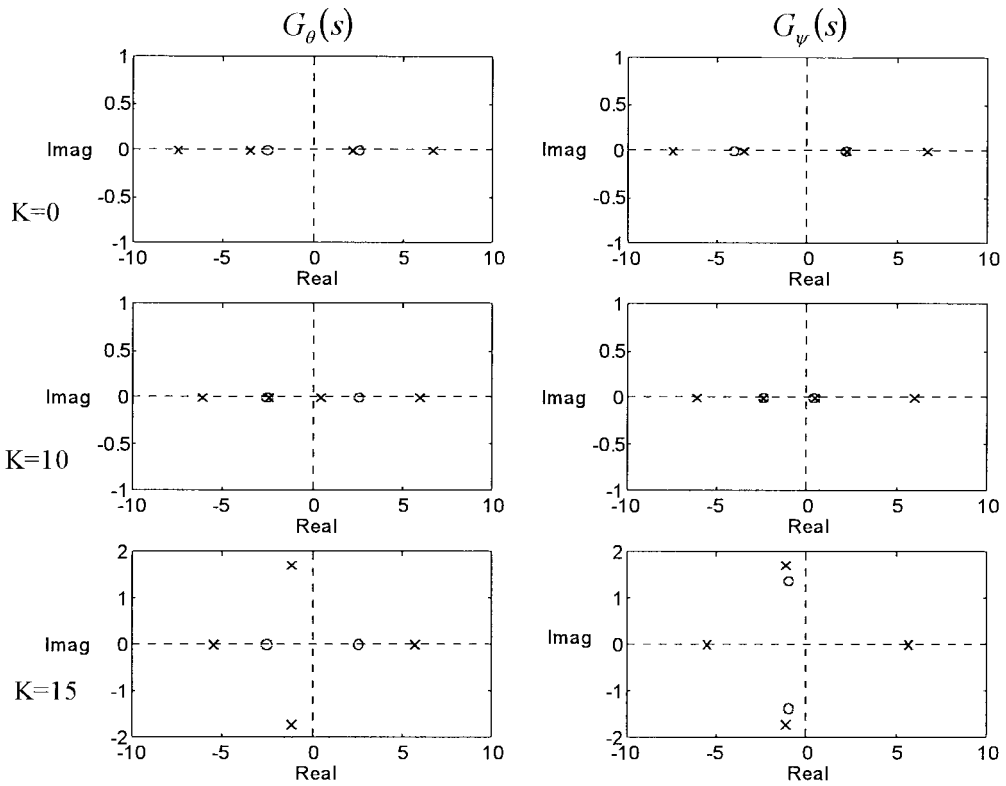

Fig. 6. The location of zeros and poles of the system, represented by two linear transfer functions G_θ and G_ψ, for the three values of ankle stiffness K which is given in [Nm/°]. It can be seen that locations of poles and zeros of the system considerably vary with different values of ankle stiffness K.

between the two RHP poles which means that no stable and minimum-phase controller can strongly stabilize this system [28]. The controller stabilizing this system has to cancel both RHP poles but the resulting closed-loop system would have unstable hidden modes. It is obvious that only an adaptive controller could be successful.[1] With the ankle joint stiffness of 10 Nm/° the configuration of zeros and poles remains the same, only that both transfer functions are "less" unstable. When the ankle stiffness is higher than $K_v = 11.2$ Nm/°, the configuration of zeros and poles changes. In $G_\theta(s)$ transfer function we still have one RHP pole and one RHP zero which means that we cannot stabilize the system only by measuring the ankle angle θ. However, the situation with $G_\psi(s)$ is more promising. One RHP pole does not represent a problem for a stable and minimum phase controller which senses only the lumbosacral angle ψ. Since $G_{\theta\psi}(s)$ is stable, when $K > K_v$, the controller stabilizes the system around both angles. This result is important for two reasons as follows:

1) with properly selected ankle stiffness we obtain a system which can be easily stabilized. Even a fixed structure controller can provide adequate robustness;
2) only the measurement of the lumbosacral angle ψ sensed by vestibular and vision system, is necessary and therefore no artificial sensors are needed.

[1] Note that the system is controllable and observable for both cases $K < K_v$ and $K > K_v$. However, in practice, the feedback stabilization of a system with $K < K_v$ is more difficult, because it requires the compensation of poles in RHP. In practice, the positions of the poles to be compensated are not exactly known and may change because of changing system characteristics (e.g., arm or head motion). Still it may be possible to compensate these poles adequately in a practical situation by using an adaptive controller. In this paper, we assume that the poles and zeros of the system are exactly known and will not further investigate the consequence of unknown or changing positions of RHP poles.

D. CNS Delay and Trunk Muscles Dynamics

Nashner [29] identified the dynamic properties of the vestibular system during perturbed standing of three normal subjects. He found that a total response time delay, associated with sensing, signal processing in the brain, and the transmission of the activation signal to the muscles, was close to 100 ms. The delay depended on the magnitude of perturbation and was higher with small perturbations. In our model the CNS dynamics was described by a pure time delay

$$G_{\mathrm{CNS}}(s) = e^{-sT_D},$$

and written in state space form

$$\begin{aligned} \dot{\underline{x}}_{\mathrm{CNS}} &= \underline{\underline{A}}_{\mathrm{CNS}}\underline{x}_{\mathrm{CNS}} + \underline{B}_{\mathrm{CNS}}u_{\mathrm{CNS}} \\ y_{\mathrm{CNS}} &= \underline{\underline{C}}_{\mathrm{CNS}}\underline{x}_{\mathrm{CNS}} + \underline{D}_{\mathrm{CNS}}u_{\mathrm{CNS}} \end{aligned} \tag{13}$$

where $G_{\mathrm{CNS}}(s)$ was approximated by a fourth order Pade equation. A simplified dynamic model of trunk flexor and extensor muscles behavior can be described by the first-order transfer function

$$G_T(s) = \frac{1}{sT_T + 1}$$

where T_T is a time constant which was found experimentally to be 0.1 s [11]. In the state space form

$$\begin{aligned} \dot{\underline{x}}_T &= \underline{\underline{A}}_T\underline{x}_T + \underline{B}_T u_T \\ y_T &= \underline{\underline{C}}_T\underline{x}_T + \underline{D}_T u_T. \end{aligned} \tag{14}$$

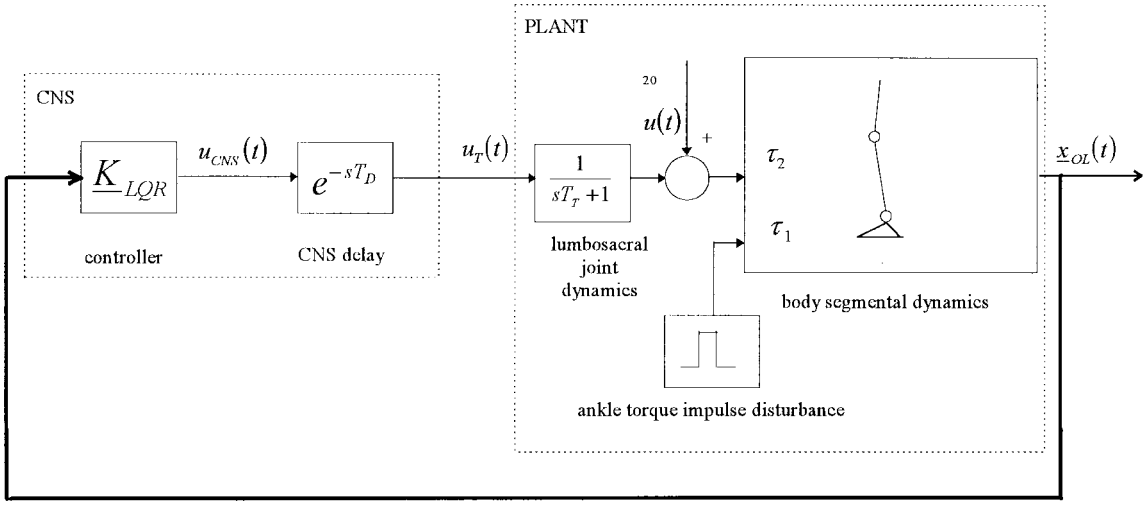

Fig. 7. The closed-loop simulation model of proposed underactuated paraplegic standing. Both angles and angular velocities are sensed by the vestibular system and vision, and proprioception of the upper body, neck and head. Calculation of the control signal representing adequate lumbosacral torque τ_2 is done by an optimal LQR controller. Time delay associated with signal sensing, processing in the brain and issuing of proper control signal to the trunk muscles is modeled as pure time delay. Actions of the controller and delay are characteristics of CNS. Delayed control signal $u_T(t)$ passes the first order filter representing isometric dynamics of trunk muscles and drives the double inverted pendulum model. τ_{20} depends on the selected posture. Ankle joint input τ_1 was augmented to the segmental dynamics model in order to enable the application of perturbation torque impulses.

The whole open-loop dynamic model is then described by the following state space equation:

$$\begin{aligned}\dot{\underline{x}}_{\mathrm{OL}} &= \underline{\underline{A}}_{\mathrm{OL}}\underline{x}_{\mathrm{OL}} + \underline{B}_{\mathrm{OL}}u_{\mathrm{CNS}}\\ y_{\mathrm{OL}} &= \underline{\underline{C}}_{\mathrm{OL}}\underline{x}_{\mathrm{OL}} + \underline{D}_{\mathrm{OL}}u_{\mathrm{CNS}}\end{aligned} \tag{15}$$

where

$$\underline{x}_{\mathrm{OL}} = \begin{bmatrix}\underline{x}_{\mathrm{CNS}}\\ \underline{x}_T\\ \underline{x}\end{bmatrix},\ \underline{\underline{A}}_{\mathrm{OL}} = \begin{bmatrix}\underline{\underline{A}}_{\mathrm{CNS}} & 0 & 0\\ \underline{B}_T\underline{\underline{C}}_{\mathrm{CNS}} & \underline{\underline{A}}_T & 0\\ [\underline{B}\underline{D}_T\underline{\underline{C}}_{\mathrm{CNS}} & \underline{B}\underline{\underline{C}}_T] & & \underline{\underline{A}}\end{bmatrix}$$

$$\underline{B}_{\mathrm{OL}} = \begin{bmatrix}\underline{B}_{\mathrm{CNS}}\\ \underline{B}_T\underline{D}_{\mathrm{CNS}}\\ \underline{B}\underline{D}_T\underline{D}_{\mathrm{CNS}}\end{bmatrix}$$

$$\underline{\underline{C}}_{\mathrm{OL}} = [\underline{D}\underline{D}_T\underline{\underline{C}}_{\mathrm{CNS}} \quad \underline{D}\underline{\underline{C}}_T \quad \underline{\underline{C}}],\ \underline{D}_{\mathrm{OL}} = [\underline{D}\underline{D}_T\underline{D}_{\mathrm{CNS}}].$$

The resulting open-loop system consists of nine states: the first four states describe the time delay approximation, the fifth state represents the trunk dynamics, and last four states correspond to the mechanical model. It is controllable and observable and depends on two variables: ankle stiffness K and neural system delay T_D.

III. Controller Design and Closed-Loop Model Simulations

In order to study the properties and limitations of a model which represents the double inverted pendulum preceded by CNS delay and the trunk muscle dynamics, we need to close the loop with a suitable controller which represents the CNS activity. Even though a natural controller shows adaptive and learning capabilities, it will be modeled by a fixed structure controller, assuming that plant parameters do not change. The analysis of the open-loop system properties showed that despite being controllable and observable, the proposed standing is difficult for feedback stabilization when the ankle stiffness value is below K_v. Nevertheless, by making the previously mentioned assumption, we employed a full state linear quadratic controller (LQR) to model postural activity for all values of ankle stiffness K, since LQR guarantees closed-loop stability for any system which is controllable and observable. The calculation of feedback gains can easily be computed with commercial software (MATLAB[2]). The control law has the following form:

$$u_{\mathrm{CNS}}(t) = -R^{-1}\underline{B}_{\mathrm{OL}}^T\underline{\underline{S}}\cdot\underline{x}_{\mathrm{OL}}(t) = -\underline{K}_{\mathrm{LQR}}^T\cdot x_{\mathrm{OL}}(t)$$

where the input $u_{\mathrm{CNS}}(t)$ minimizes the following performance criterion:

$$J = \int_0^\infty (\underline{x}_{\mathrm{OL}}^T\underline{\underline{Q}}\underline{x}_{\mathrm{OL}} + u_{\mathrm{CNS}}^T R u_{\mathrm{CNS}})dt.$$

The auxiliary matrix $\underline{\underline{S}}$ is a solution of the algebraic Riccati equation

$$0 = \underline{\underline{A}}_{\mathrm{OL}}^T\underline{\underline{S}} + \underline{\underline{S}}\underline{\underline{A}}_{\mathrm{OL}} - \underline{\underline{S}}\underline{B}_{\mathrm{OL}}R^{-1}\underline{B}_{\mathrm{OL}}^T\underline{\underline{S}} + \underline{\underline{Q}}.$$

The weighting matrix $\underline{\underline{Q}}$ and the weighting scalar R are used to determine the desired behavior of the closed-loop system. We investigated three different sets of $\underline{\underline{Q}}$ and R as follows:

1)
$$Q_{i,j} = \begin{cases}10, & i=j=6,8\\ 0, & \text{otherwise}\end{cases} \text{ and } R=1;$$

2)
$$Q_{i,j} = \begin{cases}10, & i=j=7,9\\ 0, & \text{otherwise}\end{cases} \text{ and } R=1;$$

[2]MATLAB is a registered trademark of The Math Works, Inc., Natick, MA.

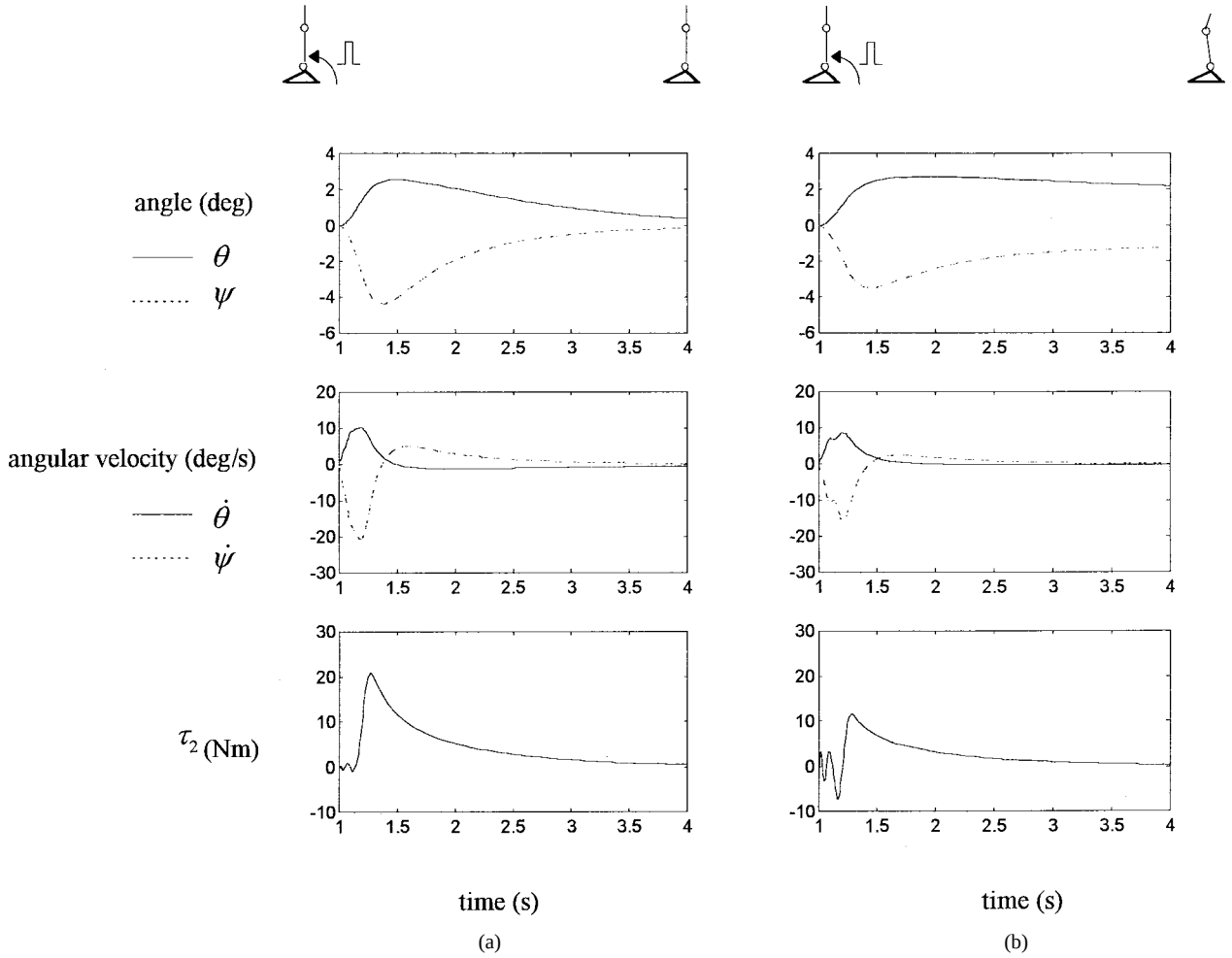

Fig. 8. Responses to the torque impulse (50 Nm, 100 ms) anterior perturbation obtained by simulation of two strategies: (a) returning to the initial posture and (b) assuming a new target posture. Upper graphs show the course of both angles, middle graphs show velocity trajectories while lower graphs display the time course of stabilizing lumbosacral torque for both cases. Stick figures on the top of the graphs represent the initial and target postures for both strategies.

3)

$$Q_{i,j} = \begin{cases} 1, & i = j = 6, 8 \\ 0, & \text{otherwise} \end{cases} \text{ and } R = 10.$$

In the first set, the angular deviations from vertical were penalized; the second set penalized angular velocities; while, in the third set, the emphasis was on the minimization of lumbosacral torque τ_2. The controller gains, computed for all three sets of weighting functions, did not differ much if $K < K_V$, while in case where $K > K_V$, the first two sets produced similar gains which were slightly different (<5%) from the third set. In the simulations, described in the following subsections, the first set of weighting matrix $\underline{\underline{Q}}$ and the weighting scalar R were used. The closed-loop simulation model is shown and described in Fig. 7. Khang and Zajac [30], [31] have proposed a closed-loop model of paraplegic standing where they simulated the recovery to upright posture from various initial states. If we assume that a paraplegic, using our control scheme, is able to maintain a selected equilibrium posture, then the only source of disturbance is the unwanted spasms around the ankle joint. Therefore, our study only simulates the responses of the closed-loop model to a torque impulse τ_1 of various amplitudes and with an arbitrarily selected duration of 100 ms. For this, a torque input is added at the ankle in (10), for the introduction of the perturbations.

A. Disturbance Rejection Strategies

It has been shown already that an underactuated system (15) has many different equilibrium states. This allows alternative balancing strategies when recovering from a disturbance. The first possible strategy of the CNS controller is to return to the initial posture after the disturbance has occurred. Another possibility is to select a new equilibrium posture—a target posture which is in the vicinity of the trajectory of the perturbed system.

We simulated the response of (15) with the following values of both system variables $K = 10$ Nm/°, $T_D = 0.15$ s for two cases as follows:

a) the initial posture was $\theta_0 = 0, \psi_0 = 0, \tau_{20} = 0$ while the target posture was the same $\theta_0 = 0, \psi_0 = 0, \tau_{20} = 0$;

b) the initial posture was $\theta_0 = 0, \psi_0 = 0, \tau_{20} = 0$ while the target posture was determined by (8), (9): $\theta_0 = 2°, \psi_0 = -1.2°, \tau_{20} = 3.6$ Nm.

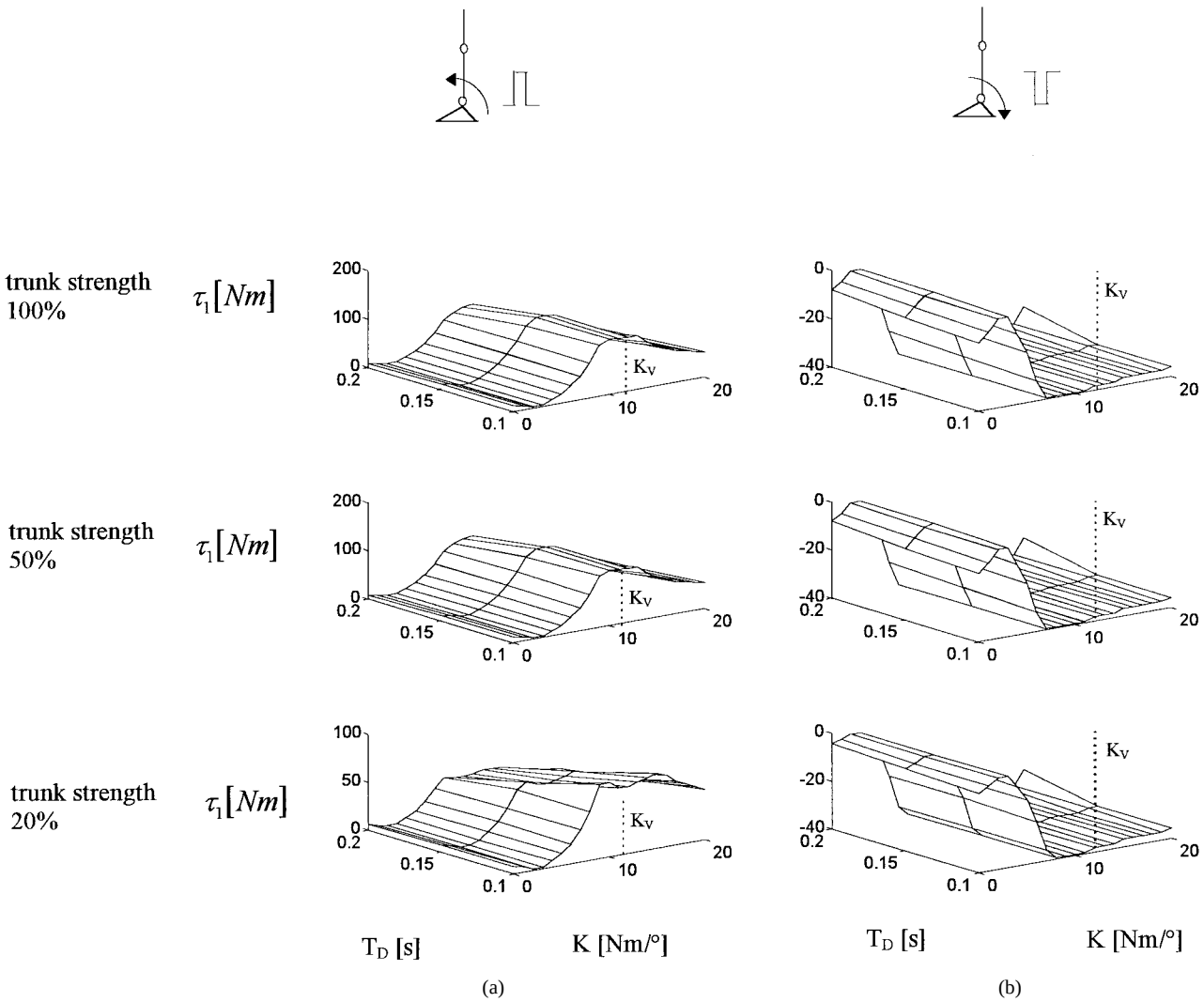

Fig. 9. Feasible ankle disturbance space for Case I. Surfaces in all six graphs represent the maximal magnitude of disturbing ankle torque impulse τ_1 (duration 100 ms), which can be rejected without violating constraints C1–C5; (a) results for three values of trunk strength in case of anterior disturbances and (b) results for three values of trunk strength in case of posterior disturbances.

In case b), the posture after perturbation was selected arbitrarily. Any other equilibrium posture could be assumed instead. The torque impulse $\tau_1 = 50$ Nm of 100 ms duration, was applied at the first second of the simulation run. From the response shown in Fig. 8, we see that the peak values of θ are similar for both cases, while the peak excursion of ψ is lower in the second case. The peak values of both angular velocities are lower in the second case and the peak value of lumbosacral torque in the first case is almost twice as large as in the second case. The oscillations in the first 200 ms of the lumbosacral torque τ_2 are due to the Pade approximation of the neural system time delay. The simulations presented in the paper were performed by MATLAB[2] SIMULINK[3] software.

From these results, we can see that a paraplegic while balancing in this way, has many options when recovering from disturbances. By selecting the proper strategy, he can minimize the lumbosacral torque needed for stabilization.

[3] SIMULINK is a registered trademark of The Math Works, Inc., Natick, MA.

B. Feasible Perturbation Space Determination

An important question, which needs to be answered, concerns the optimal value of the ankle stiffness. Which value of K makes the system (15) optimal in a sense that it tolerates maximal disturbances in the presence of constraints (C1–C4) and various neural system delays T_D. Additionally, we wish to investigate the system behavior for all three posture groups, therefore, we will examine the closed-loop (15) properties for the following three cases:

I) "upright" posture where $\theta_0 = 0$;
II) "forward" posture where $\theta_0 = 2°$;
III) "backward" posture where $\theta_0 = -2°$.

For each case the simulations for positive and negative ankle torque disturbances were performed (impulse duration 100 ms). The constraint C3 was set to three different values: 100, 50, and 20% of the trunk strength assessed in a normal subject. Thus, each case is represented by six different examples, where the feasible disturbance space was determined for ankle stiffness values ranging from 0 to 20 Nm/° and for three values of the neural system delay (0.1, 0.15, and 0.2 s). We have

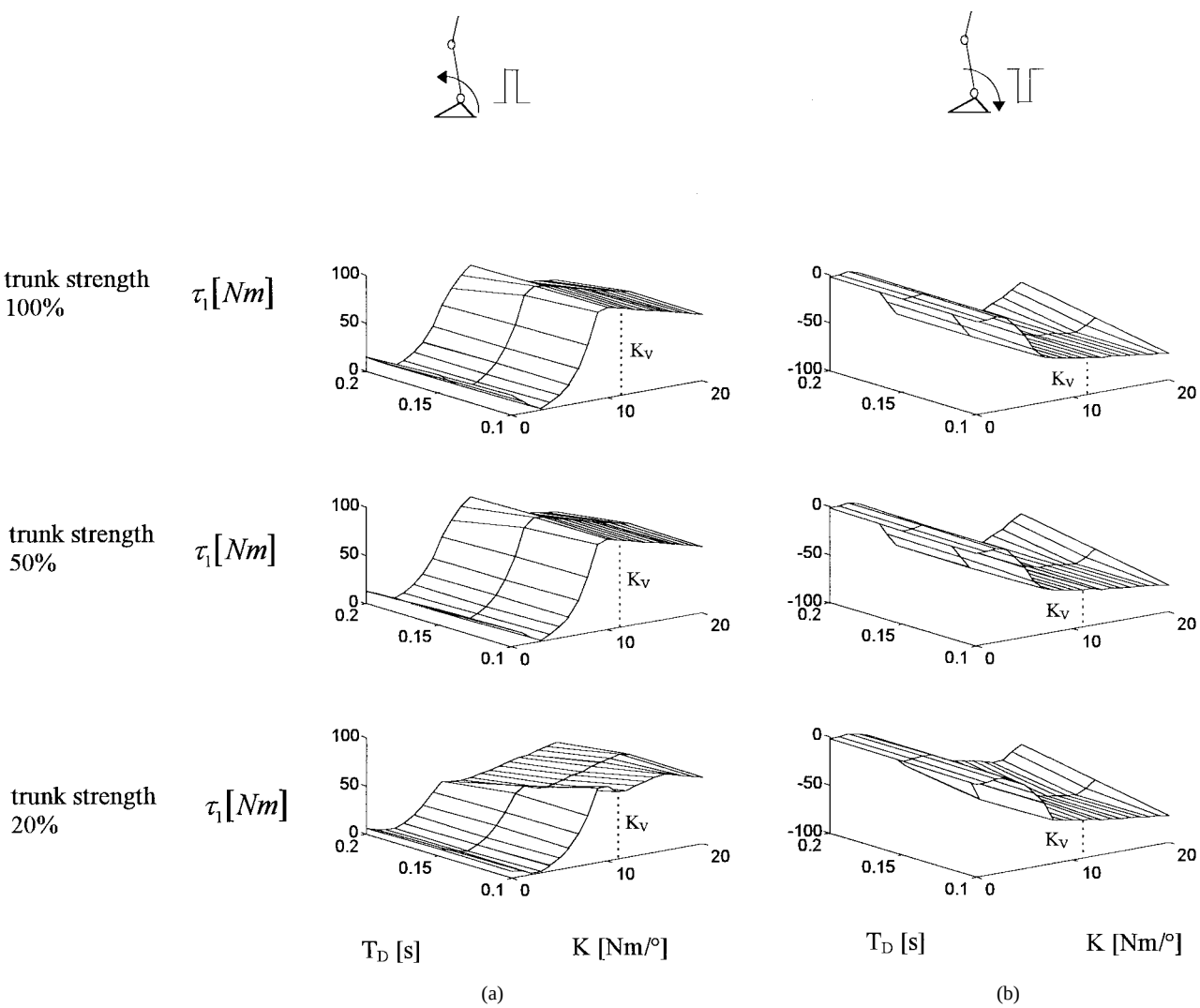

Fig. 10. Feasible ankle disturbance space for Case II. Surfaces in all six graphs represent the maximal magnitude of disturbing ankle torque impulse τ_1 (duration 100 ms), which can be rejected without violating constraints C1–C5: (a) results for three values of trunk strength in case of anterior disturbances and (b) results for three values of trunk strength in case of posterior disturbances.

additionally imposed a constraint on the absolute values of both angles θ and ψ which had to remain within the range of 10° (C5). This constraint was needed at very low values of ankle stiffness (from 0 to 3 Nm/°) where the resulting trajectories, for which the linear model is no longer valid, do not violate the first four constraints. Disturbance rejection strategy a), explained in the previous subsection, was utilized in simulations of all three cases.

Fig. 9 shows the results for an upright standing posture (Case I). Surfaces in all six graphs represent the maximal values of the disturbance torque impulse τ_1 which can be rejected without violating constraints C1–C5. The optimal value of the ankle stiffness for perturbations in the anterior direction is around K_V. The major constraint for anterior disturbances is C1, i.e., the length of the foot. Only for stiffness values from 0 to 3 Nm/° is constraint C5 dominant. For negative perturbations, we see an interval of ankle stiffness from 8 to 18 Nm/°, where the performance of the system is similar. The influence of the constraints is similar for posterior as for anterior disturbances. It is interesting that the trunk strength constraint (C3) does not have a major impact on the abilities of the underactuated double inverted pendulum to reject disturbances. In the case of anterior disturbances, only in the third example (20% trunk strength) is the feasible disturbance space reduced by 50%, while in case of posterior disturbances, trunk strength does not have any influence. The influence of increased time delay has little effect on the feasible disturbance space, however, it does have an influence on maximal lumbosacral torques τ_2 required for balancing.

For Case II (Fig. 10), similar conclusions can be drawn for anterior disturbances as in Case I. The optimal value of stiffness is K_V while the feasible disturbance space is now slightly reduced. However, this optimum is not as sharp as in Case I and values of stiffness higher than K_V are also acceptable. The optimal stiffness value for posterior disturbances is 18 Nm/° while the feasible disturbance space is significantly greater than in Case I. Different trunk strengths and neural system delays have similar influence as in Case I.

For Case III (Fig. 11), we have a sharp optimal ankle stiffness for both disturbance directions, which is in both cases

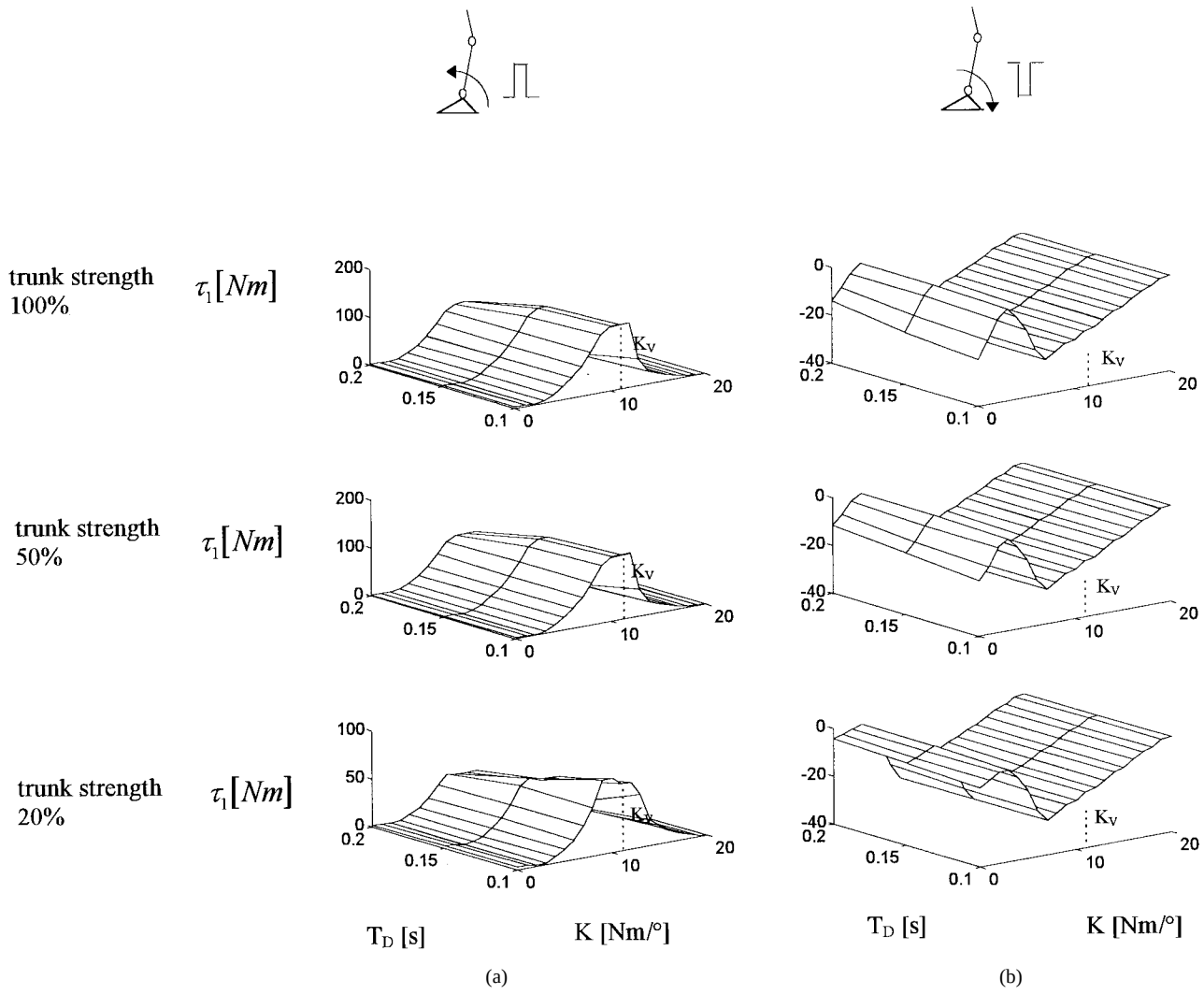

Fig. 11. Feasible ankle disturbance space for Case III. Surfaces in all six graphs represent the maximal magnitude of disturbing ankle torque impulse τ_1 (duration 100 ms), which can be rejected without violating constraints C1–C5: (a) results for three values of trunk strength in case of anterior disturbances and (b) results for three values of trunk strength in case of posterior disturbances.

close to K_V. The feasible disturbance space for posterior-directed disturbances is smaller than in Case I and even more in regard to Case II, while the size of the feasible disturbance space, for disturbances acting in an anterior direction, is comparable to the previous two cases. The influence of trunk strength and neural system delay is also similar to the previous two cases as well as the action of the constraints.

IV. Discussion

We believe that demonstrating the existence of the ankle stiffness K_V where 1) the equilibrium angle of the lumbosacral joint is independent of the selected ankle angle, 2) the dynamic properties of the system are significantly changed (favorable zero-pole locations), and 3) the system can tolerate maximal torque impulse disturbances without violating constraints (C1–C5), is the most important contribution of this theoretical study. From the results presented in Part I, we expect that a subject, standing with ankle stiffness $K > K_V$, will have little difficulty with balancing since we are sure that the CNS can act as a fixed-parameter controller. If $K < K_V$, it is not clear from theory whether the subject will be able to balance or not. The analysis of zero-pole locations of the open-loop system suggests that adaptive control is necessary. However, in Part II, we demonstrate experimentally that this is possible. The simulations showed that the most significant constraint is the length of the foot (C1), which, to a great extent, determines the feasible disturbance space for the various different postures. The feasible disturbance space was determined by simulation for various system conditions, but only for the balancing strategy where the subject returns into the initial position. If, instead, a new target posture is assumed, following the application of disturbance, the feasible disturbance space increases in all cases.

The existence of different disturbance rejection strategies is a very important finding because it enables voluntary posture switching. We introduced three different postures: upright-, forward-, and backward-leaning. It is unlikely that the paraplegic would be able to maintain the exact upright posture, because the system is inherently unstable and needs continuous active balancing. It is more likely that a subject

will switch between the forward and backward posture. As Kralj *et al.* [4] pointed out, many different postures exist, in which stimulation of different muscle groups is needed to maintain the knees and hips in extended positions. On the other hand, in some postures, the same effect can be obtained passively. Thus, by changing between different postures, the fatigue rate of the knee and hip extensors can probably be reduced by switching on and off their stimulation as required for the voluntary-selected current posture. These switchings should occur gradually in order to have a negligible impact on the balance. Note that there is also no need to change a reference for the artificial controller of the ankles when the subject switches his posture.

It is also interesting to compare the optimal value of ankle stiffness K_V with the passive stiffness assessed in the paraplegic subject [9]. The stiffness at zero background torque for both ankles was found to be 6 Nm/°. Additional stiffness of 5 Nm/° needed to reach K_V can be produced either by FES of ankle muscles or, even more promising, by passive springs mounted in both shoes. The passive solution efficiently solves all the problems regarding measurements of the ankle angle and position of the COP that are needed in the closed-loop FES stiffness control.

Another interesting result of this theoretical study is that the preserved sensors (vestibular system, vision) might be sufficient for successful balancing, since only the measurement of the lumbosacral angle ψ was found to be needed by the CNS. However, it is unlikely that the intact natural senses can provide adequate information about the ankle angle to tell the subject which posture is being assumed. In this respect, cognitive sensory feedback, providing the information about the current posture, might be valuable. If the ankle stiffness is provided by FES of ankle dorsal- and plantar-flexors, cognitive feedback may also provide information about the fatigue of dorsiflexors while standing in a backward posture, and plantar-flexors during standing in a forward posture. In this way, the standing subject would know when to switch between the postures. We demonstrate this in Part II.

In our theoretical study we made several assumptions. The most important assumption was the symmetry of both legs, which were lumped together into a single link in our mechanical model. This assumption was needed in order to study the postural activity only in the sagittal plane. Clearly, no such symmetry exists in paralyzed limbs since fatiguing and spasms in both legs may be significantly different, leading also in the lateral movement and rotation of the body. In the discussion of Part II, we propose a solution that might circumvent this difficulty. In our simulations we also studied the responses of a closed-loop model to ankle torque impulses of various amplitudes, and duration of 100 ms. Torque impulses due to spasticity are often longer than 100 ms. However, longer durations of disturbance impulse will significantly reduce the feasible disturbance space, while the shape of surfaces presented in Figs. 9–11 remain similar. In case of a high torque and a long duration of spasm, the paraplegic would have to use his arms in order to prevent falling.

Theoretically, the underactuated systems are usually very difficult to control because they generally require very large input signals [15] to control both the active and passive degrees of freedom. By adding artificial stiffness in the passive ankle joints, we reduced the need for such large input signals at the active lumbosacral joint. The price we had to pay is the limited repertoire of the equilibrium states. However, in posture control, this is not an important deficiency as the space is anyway quite narrow. The unexpected result of the simulation study is the finding that the trunk strength is not of major importance for successful underactuated standing since the other constraints (primarily C1) become active first. This enlarges the potential population of paraplegic subjects who are candidates for arm-free FES standing.

V. Conclusion

A novel control strategy for unsupported paraplegic standing was proposed. The approach integrates the residual sensory and motor abilities of paraplegic subjects with the FES orthotic device in a manner that provides arm-free standing. Experiments are described in Part II.

Acknowledgment

The authors are indebted to Dr. N. Donaldson who significantly improved the English of this paper.

References

[1] A. Kralj and T. Bajd, *Functional Electrical Stimulation: Standing and Walking After Spinal Cord Injury*. Boca Raton, FL: CRC Press, 1989.
[2] P. W. Axelson, D. Gurski, and A. Lasko-Harvill, "Standing and its importance in spinal cord injury management," in *Proc. 10th Annu. Conf. Rehab. Tech. RESNA'87*, San Jose, CA, 1987, pp. 477–479.
[3] H. J. Chizek, "Adaptive and nonlinear control methods for neural prostheses," in *Neural Prostheses*, R. B. Stein, P. H. Peckham, and D. B. Popović, Eds. Oxford, U.K.: Oxford University Press, pp. 298–327, 1992.
[4] A. Kralj, T. Bajd, R. Turk, and H. Benko, "Posture switching for prolonging functional electrical stimulation standing in paraplegic patients," *Paraplegia*, vol. 24, pp. 221–230, 1986.
[5] H. J. Chizeck, R. Kobetic, E. B. Marsolais, J. J. Abbas, I. H. Donner, and E. Simon, "Control of functional feuromuscular stimulation systems for standing and locomotion in paraplegics," *Proc. IEEE*, vol. 76, pp. 1155–1165, 1988.
[6] A. J. Mulder, P. H. Veltink, H. B. K. Boom, and G. Zilvold, "Low-level finite state control of knee joint in paraplegic standing," *J. Biomed. Eng.*, vol. 14, pp. 3–8, 1992.
[7] R. J. Jaeger, "Design and simulation of closed-loop electrical stimulation orthoses for restoration of quiet standing in paraplegia," *J. Biomech.*, vol. 19, pp. 825–835, 1986.
[8] N. de N. Donaldson, "Practical ankle controllers for unsupported standing in paraplegia," in *Proc. Ljubljana FES Conf.*, Ljubljana, Slovenia, 1993, pp. 61–64.
[9] M. Munih, K. Hunt, N. Donaldson, and F. M. D. Barr,"LQG moment control in the paraplegic's ankle joint," in *Proc. IEEE-EMBS*, Amsterdam, The Netherlands, 1996, p. 57.
[10] M. Munih, K. Hunt, and N. Donaldson, "LQG control for the ankle joint moment," in *Proc. 9th ICMMB*, Ljubljana, Slovenia, 1996, pp. 151–154.
[11] Z. Matjačić, T. Bajd, M. Gregorič, H. Benko, and P. Obreza, "Trunk muscles strength evaluation in normal and paraplegic subject," in *Proc. 9th ICMMB*, Ljubljana, Slovenia, 1996, pp. 437–440.
[12] N. A. Langrana and C. K. Lee, "Isokinetic evaluation of trunk muscles," *Spine*, vol. 9, pp. 171–175, 1984.
[13] L. M. Nashner and G. McCollum, "The organization of human postural movements: A formal basis and experimental synthesis," *Behav. Brain Sci.*, vol. 8, pp. 135–172, 1985.
[14] F. B. Horak and L. M. Nashner, "Central programming of postural movements: Adaptation to altered support-surface configurations," *J. Neurophys.*, vol. 55, pp. 1369–1381, 1986.

[15] C. L. Golliday, Jr. and H. Hemami, "Postural stability of the two-degree-of-freedom biped by general linear feedback," *IEEE Trans. Automat. Contr.*, vol. AC-21, pp. 74–79, 1976.
[16] H. Koozekanani, K. Barin, R. B. McGhee, and H. T. Chang, "A recursive free body approach to computer simulation of human postural dynamics," *IEEE Trans. Biomed. Eng.*, vol. BME-30, pp. 787–792, 1983.
[17] K. Barin, "Evaluation of a generalized model of human postural dynamics and control in sagittal plane," *Biologic. Cybern.*, vol. 61, pp. 37–50, 1989.
[18] H. Hemami, F. C. Weimer, C. S. Robinson, C. W. Stockwell, and V. Cvetkovic, "Biped stability considerations with vestibular models," *IEEE Trans. Automat. Contr.*, vol. AC-23, pp. 1074–1079, 1978.
[19] H. Hemami, F. C. Weimer, and S. H. Koozekanani, "Some aspects of the inverted pendulum problem for modeling of locomotion systems," *IEEE Trans. Automat. Contr.*, vol. AC-18, pp. 658–661, 1973.
[20] L. M. Nashner, "Vestibular and reflex control of normal standing," in *Control of Posture and Locomotion*, R. B. Stein, K. G. Pearson, R. S. Smith, and J. B. Redford, Eds. New York: Plenum, 1973, pp. 291–308.
[21] A. D. Kuo, "An optimal control model for analyzing human postural balance," *IEEE Trans. Biomed. Eng.*, vol. 42, pp. 87–101, 1995.
[22] D. A. Winter, *Biomechanics of Human Movement.* New York: Wiley, 1979.
[23] A. D. Kuo and F. E. Zajac, "A biomechanical analysis of muscle strength as a limiting factor in standing posture," *J. Biomechan.*, vol. 26, supp. 1, pp. 137–150, 1993.
[24] T. Sinkjaer and I. Magnussen, "Passive, intrinsic, and reflex-mediated stiffness in the ankle extensors of hemiparetic patients," *Brain*, vol. 117, pp. 355–363, 1994.
[25] A. Trnkoczy, T. Bajd, and M. Maležič, "A dynamic model of the ankle joint under functional electrical stimulation in free movement and isometric conditions," *J. Biomechan.*, vol. 9, pp. 509–519, 1976.
[26] M. Bergerman, C. Lee, and Y. Xu, "A dynamic coupling index for underactuated manipulators," *Journal of Robotic Systems*, vol. 12, pp. 693–707, 1995.
[27] M. W. Spong, "Partial feedback linearization of underactuated mechanical systems," in *Proc. IEEE-IROS Conf.*, Munich, Germany, 1994, pp. 314–321.
[28] S. Skogestad and I. Postlethwaite, *Multivariable Feedback Control.* New York: Wiley, 1996.
[29] L. M. Nashner, "A model describing vestibular detection of body sway motion," *Acta Otolaryng.*, vol. 72, pp. 429–436, 1971.
[30] G. Khang and F. E. Zajac, "Paraplegic standing controlled by functional neuromuscular stimulation: Part I—Computer model and control-system design," *IEEE Trans. Biomed. Eng.*, vol. 36, pp. 873–884, 1989.
[31] G. Khang and F. E. Zajac, "Paraplegic standing controlled by functional neuromuscular stimulation: Part II—Computer simulation studies," *IEEE Trans. Biomed. Eng.*, vol. 36, pp. 885–894, 1989.

Zlatko Matjačić received the B.Sc., M.Sc., and D.Sc. degrees from the Faculty of Electrical Engineering, University of Ljubljana, Slovenia, in 1992, 1995, and 1998, respectively.

He was a Research and Teaching Assistant at the Department of Electrical Engineering, University of Ljubljana and is presently an Assistant Professor of Biomedical Sciences and Engineering at the Center for Sensory-Motor Interaction, Aalborg University, Denmark. His research interests include human motion analysis and synthesis, biomechanics, and control of human motion.

Tadej Bajd (SM'91) received the B.Sc., M.Sc. and D.Sc. degrees from the Faculty of Electrical Engineering, University of Ljubljana, Slovenia, in 1972, 1976, and 1979, respectively.

He was a Research Assistant at the J. Stefan Institute, Ljubljana, and a Visiting Research Fellow at the University of Southern California, Los Angeles, and Strathclyde University, Glasgow, Scotland. He is currently Professor of Robotics at the Department of Electrical Engineering, University of Ljubljana. He is the author and coauthor of 50 journal papers in the field of biomedical engineering and robotics.

Dr. Bajd has received the Slovene National Award for his scientific achievements in the field of functional electrical stimulation for paralyzed subjects. He is President of the Slovene Society for Medical and Biological Engineering, a member of IFMBE and a member of the Council of the ESEM.